Research Article

Nano Biomed Eng

Piperine Loaded Titanium Dioxide Nanoparticles: Development,Characterisation and Biomedical Application

Ahmed Talib Yassen[1], Khalisa K. Khudair[2], Marwa Abdul Muhsien Hassan[3]

[1]Department of Physiology / College of Medicine / University of Anbar, Iraq.
[2]Department of Physiology, Biochemistry and Pharmacollogyl / College of Veterinary Medicine / University of Baghdad, Iraq.
[3]Department of Physics / College of Science / Mustansiriyah University / Baghdad, Iraq.

Corresponding authors. E-mail: marwamedicalphysics@uomustansiriyah.edu.iq; marwamedicalphysics@gmail.com

Received: Sep. 27, 2021; **Accepted:** Oct. 10, 2022; **Published:** Nov. 17, 2022

Citation: Ahmed Talib Yassen, Khalisa K. Khudair, and Marwa Abdul Muhsien Hassan,Piperine Loaded Titanium Dioxide Nanoparticles: Development, Characterisation and Biomedical Application. *Nano Biomed. Eng*., 2022, 14(2): 192-200.
DOI: 10.5101/nbe.v14i2.p192-200.

Abstract

TiO_2 nanoparticles were prepared by using electrochemical anodization method. UV-Vis absorption spectrum of TiO_2 and TiO_2: piperine nanoparticles have an absorption edge in the range of (340 -355) nm, suggesting that the TiO_2 colloidal obtained is anatase phase. The band gap energy (E_g) for TiO_2 nanoparticles (3.46 eV) is higher than the value of (3.20 eV) for bulk TiO_2. X-Ray diffraction results for TiO_2 nanoparticles with a wavelength of 1.54 Å were investgation in this work. Planes (101), (200), (111), (220), (210), (211), (105), (220), (310), (221), and (220) crystal planes all had peaks with the lattice constants a = 3.755 Å and c = 9.5114 Å confirms the anatase phases of the TiO_2 nanoparticles according to the JCPDS file 21-127231. Scanning Electron Microscope images of TiO_2 samples in revealed the prevalence spherical nanosized crystallites, where clear nanostructures with a grain size of 15 nm. In TEM image, the shape of the nanoparticles was spherecial, with small size variance and found to be 15 nm. The EDX study of the nanoparticle reflects the atomic percentage of elements such as Ti and O with a ratio of 83:17 and no other peaks are observed this confirm the presence of TiO_2 nanoparticles.

Keywords: TiO_2, TiO_2: piperine, SEM, Optical properties

Introduction

Piperine, a dietary polyphenol isolated from black and long peppers, distinguished with its intrinsic features, does not only improve curcumin's existing anti-cancer activity, but also its extremely poor bioavailability (Teiten *et al.*, 2010; Patial *et al.*, 2015; Tang *et al.*, 2017). Besides, piperine alone possesses anti-mutagenic and anti-tumor influences (Srinivasan, 2007; Chinta *et al.*, 2015). Piperine has been widely reported to inhibit the growth of colon cancer cell lines by G1 arrest in cell cycle and by triggering apoptosis (Yaffe *et al.*, 2015), and to enhance exhibition of antitumor activities in prostate cancer (Ouyang *et al.*, 2013). Despite the proven antitumor activities of curcumin and piperine, the low solubility and the poor chemical stability of the compounds in water, largely limit their clinical applications. Targeted and triggered drug delivery systems accompanied by nanoparticle technology have been investigated as a prominent strategy to address these limitations (Bisht and Maitra, 2009; Ucisik *et al.*, 2013b; Yallapu *et al.*, 2013; Purpura *et al.*, 2018; Wong *et al.*, 2019). Polymeric nanoparticles (Anand *et al.*, 2010; Bisht

et al., 2010; Mahmood *et al.*, 2015; Pachauri *et al.*, 2015), cyclodextrin nanoparticles (Ndong Ntoutoume *et al.*, 2016; Dash and Konkimalla, 2017b), liposomes (Li *et al.*, 2005; Dutta and Bhattacharjee, 2017), mixed and copolymeric micelles (Gou *et al.*, 2011; Wang *et al.*, 2012; Li *et al.*, 2015; Hevus *et al.*, 2017), and solid lipid nanoparticles (Ucisik *et al.*, 2013b; Jourghanian *et al.*, 2016) are among the mostly applied curcumin and piperine nanoformulations (Naksuriya *et al.*, 2014; Mahran *et al.*, 2017). As a lipid-based, safe and surfactant-free system, emulsomes emerge as a promising drug delivery system among the alternatives [1]. TiO_2 exists in three different crystalline habits: rutile (tetragonal), anatase (tetragonal) and brookite (orthormbic). Both anatase and rutile have tetragonal crystal structure but belong to different phase groups. Anatase has the space group I41/ amd [4] with four formula units in one unit cell and rutile has the space group P42/ mnm [2] with two TiO_2 formula units in one unit cell [3]. The low- density solid phases are less stable and undergo transition rutile in the solid state. Rutile TiO_2 has some advantages over anatase phase, such as higher refractive index, higher dielectric constant, higher electric resistance and higher chemical stability. The transformation is accelerated by heat treatment and occurs at temperture degrees in the range of (450-1200) °C [4]. This transformation is dependent on several parameters such as initial particle size, initial phase, dopant concentration, reaction atmosphere and annealing temperture [5, 6]. Among several metal oxide nanoparticles, titanium dioxide nanoparticles (TiO_2 NPs) are non-toxic with oxidation potency and elevated stability to light resulting into their broad applications in environmental remediation [7, 8]. In addition, TiO_2 NPs possess fascinating dielectric, optical, antimicrobial, chemical and catalytic properties which lead to industrial applications such as cosmetics, pigment, fillers, whitening and brightening of foods, in personal care products like toothpaste, and photocatalyst [9-14]. The vital applications of nano TiO_2 are photocatalytic degradation and splitting; PV cells, electrochromic and electronic devices, and sensing instruments have heartened huge interest and widespread advancement for synthesis of TiO_2 NPs [15-18]. TiO_2 NPs have been widely used in daily life and can be synthesized through various physical, chemical, and green methods [19]. Various chemical synthesis techniques are largely employed for the synthesis of TiO_2 nanoparticles such as sol-gel method [20], solvo-thermal method [21] co precipitation method [22], and hydrothermal method [23]. Green TiO_2 NPs have good points rather than chemically synthesized NPs as they have a good antifungal as well as antimicrobial activity [24-26].

The purpose of the present manuscript is the determination of an improved chemical synthesis of TiO_2 NPs using piperine with conditions that could be easily reproducible in industry, both in terms of energy saving and cost reduction.

Experimental

Experimental Section

Titanium Tetrachloride $TiCl_4$ 99.99% and absolute ethanol CH_3CH_2OH 99.99% for producing TiO_2 nanoparticles by adding drop wise from $TiCl_4$ in ethanol with 1:10 ratio under centrifuge with 8 hour. The reaction was performed at room temperature while stirring under fume hood due to the large amount of Cl_2 and HCl at 30 min. The solution was left to rest and cool back at room temperature for 2 hour, then after that measured the pH of the solution in the range of (1-2). Before electrochemical anodization, titanium (Ti) foils (250 μm thick, purity 97%) with a size of 1 cm×2.5 cm were degreased by ultra-sonication in a mixture (15 mL) for each one of acetone, methanol, and methylene chloride for 30 min, followed by washing with a large amount of distilled water and drying with N_2. Electrochemical anodization was carried out in a two-electrode cell using a power source PS-3030, where the Ti foil was used as the anode and cathod electrode after annealing at 800 °C for 4 hour. Anodization electrolytes were fabricated by using above solution TiO_2 with 30 volt. Each potential static anodization was performed under the room temperature of ~23 °C, after a certain period of anodization, 2 hour; The final solution was dried at 80 °C until powder was formed. The obtained TiO_2 powder was calcined for two hours in the box furnace at 500 °C in an ambient atmosphere in this temperature getting TiO_2 nanoparticles in anatase phase when increasing the temperature degree to 900 °C the phase transformation from anatase to rutile in TiO_2 powder [27]. TiO_2: piperine nanostructure construction using (2.5 gm in 50 mL distilled water) of TiO_2 nanoparticles droped in (2.5 gm in 50 mL distilled water) Piperine ratio 50:50 mL.

Measurements and characterization

X-Ray diffraction (XRD) pattern

In order to explain the structural properties, the nature and the crystal growth of TiO_2 nanoparticles,

X-ray diffraction measurement was carried out done according to the ASTM (American Society of Testingn Materials) cards, using (Philips pw 1050 X-ray diffractometer of 1.54 Å from Cu-kα, Japan). Cu radiation source, at a scanning speed of 2 min^{-1}, 40 kV tube voltage, and 30 mA tube current.

The crystallinity of synthesized material, the average particle (green) size (Dg) of TiO_2 NPs has mostly calculated by using the Debye–Scherrer's equation after the successful synthesis [28, 29]. The Scherrer's equation is considered as the most fundamental and widely used equation to calculate the particle size by the combination of 2θ and FWMH values from the XRD data.

$$D = K\lambda\beta\cos\theta \quad (1)$$

In this equation, D represents the Particle size (Diameter), K is Scherrer's constant (0.9), λ = 0.15406 nm (Wavelength of X-ray source), β represents Full width at Half-maximum intensity (FWHM) in radians and q is used to denote the Peak positions in (Radians), and θ is the Bragg's diffraction angle of the respective XRD peak.

Scanning electron microscopy and energy dispersive spectroscopy (EDSX)

The scanning electron microscope (SEM) is a type of electron microscope using an electron beam energy of 15 keV and a beam current of 2.62 A. The SEM study has been carried out by Hitachi (S-4160) scanning electron microscope the magnification power continuous form 6x to 100,000x. The setting in thin film laboratory at University of Tehran. Scanning electron microscopy (SEM) images of the same samples were recorded with a LED-1430VP microscope using an electron beam energy of 15 keV and a beam current of 2.62 A.

Transmission electron microscopy

Transmission Electron Microscope ((TEM) JEOL JEM 1400, Japan) was used for investigating the size and shape of nanoparticles.

Optical properties measurements

Optical transition measurement: A double-beam (UIR-210A spectrophotometer from Shimadzu, Japan) was used in order to record the optical transmission and absorption spectra of the TiO_2 nanoparticles within the wavelength range (300-900 nm). It is generally used for characterizing various metal nanoparticles in the size range of 2-100 nm and more [30, 31]. The optical band gap was estimated graphically by applying the Tauce model; the band gap of the prepared material with sharp fall off can be deduced from a plot of the squared absorption coefficient $(\alpha h\upsilon)^2$ versus photon energy (hυ) by extrapolating the straight line of the plot to intersect the energy axis. UV-vis absorption measurements were recorded on UV-vis Spectrophotometer-UVD-3200 (LABOMED, Los Angeles, CA, USA). Furthermore, UV-vis spectrum of TiO_2 is used to calculate the band gap energy (E_g) using well known Tauc's equation [32, 33].

$$\alpha h\nu = A(h\nu - E_g) \quad (2)$$

Where α: absorption coefficient, h: Planks constant (6.626×10^{-34} J s), ν: light frequency, A: constant, E_g: optical band gap energy value of the semiconductor TiO_2.

FTIR measurement

Fourier Transform-Infrared Spectroscopy (FTIR) probes the molecular vibrations of molecules. Light of different energies (or frequency, represented by wavenumbers in the spectrum above) is directed through a sample. When a particular energy (or freguency) of light matches a vibrational frequency of the molecule, the molecule absorbs the light and vibrates. Peaks in an infrared spectrum are upside-down compared to other forms of spectroscopy to convey that the peak is a decreased intensity, or absorbance of light. The (SHIMADZU- 8400S, Koyoto, Japan) Scan of the FTIR measurements are performed over the range between (400-4000) cm^{-1} for the prepared sample.

Results and Discussions

X-Ray diffraction results for TiO_2 nanoparticles

Figure 1 shows the X-Ray diffraction results for TiO_2 nanoparticles using X-rays with a wavelength of 1.54 Å. Planes (101), (200), (111), (220), (210), (211), (105), (220), (310), (221), and (220) crystal planes all had peaks with the lattice constants a = 3.755 Å and c = 9.5114 Å confirms the anatase phases of the TiO_2 nanoparticles according to the JCPDS file 21-1272 31. X-ray diffraction profiles are usually influenced by crystallite size and lattice strain. The fact that the crystalline sizes of the samples are very small causes the peaks to broaden. Moreover, the intensities difraction peak decreases and becomes broader for TiO_2: piperine nanoparticles indicating smaller particle size [34], which is important for quality and decreasing

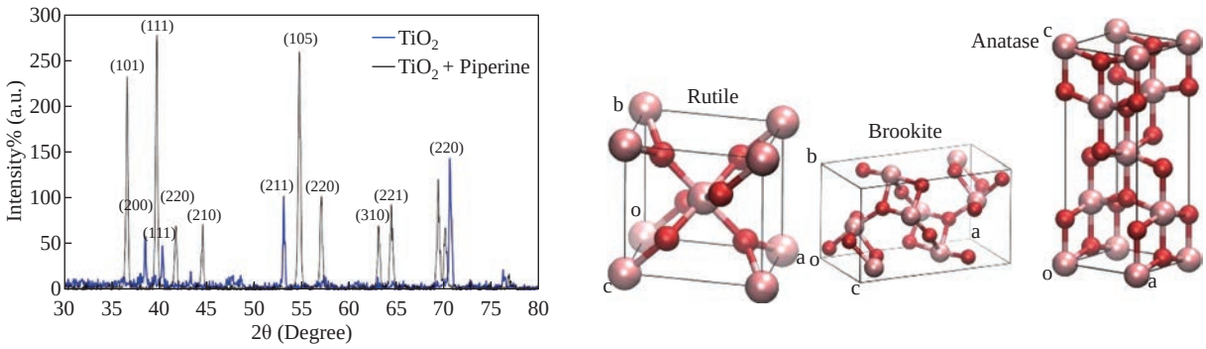

Fig. 1 X-Ray diffraction results for TiO_2 and TiO_2: piperine nanoparticles.

Table 1 Organ index of Brain, Heart, liver and kidneys of mice exposed to TiO_2: Piperinefor 60 days compared with normal organs obtained from the control mice

	Organ index, Mean ± SD							
groups	Brain	P value	Heart	P value	Liver	P value	kidney	P value
Control	0.93 ± 0.058	$p > 0.05$	1.01 ± 0.064	$p > 0.05$	1.26 ± 0.048	$p > 0.05$	1.04 ± 0.049	$p > 0.05$
2 mg/mL	0.95 ± 0.053	$p > 0.05$	1.20 ± 0.055	$p > 0.05$	1.11 ± 0.057	$p > 0.05$	1.13 ± 0.059	$p > 0.05$
4 mg/mL	1.12 ± 0.065	$p > 0.05$	0.95 ± 0.049	$p > 0.05$	1.13 ± 0.054	$p > 0.05$	0.94 ± 0.066	$p > 0.05$
6 mg/mL	1.12 ± 0.058		0.96 ± 0.050		1.15 ± 0.057		1.10 ± 0.063	

TiO_2 tixiocity.

LD50 measurement of nanoparticles toxicity for 60 days was measured after observing the number of dead mice. Changes in the weight of the mice and its organs including Brain, Heart, liver and kidneys were evaluated due to the administration of various doses of the TiO_2: Piperine nanostructure according to the organ index formula:

$$\text{Organ Index} = \frac{\text{Wt. of experimental organ / Wt. of the experimental mice}}{\text{Wt. of control organ / Wt. of the control mice}} \quad (3)$$

Scanning Electron Microscope (SEM) images of TiO_2 samples

Scanning Electron Microscope (SEM) images of TiO_2 nanoparticles are shown in Fig. 2(a) and 2(b). Clear nanostructures with a grain size of 15 nm can be observed. The TiO_2 nanoparticles seen in the SEM picture clearly contain a number of crystallites (see Fig. 2(a)). The grain size of TiO_2 nanoparticles characterized in XRD-Diffractometer by Debye-Sherrer equation is smaller than the results observed by SEM as compared to XRD results. As the solution stringed in a short time, the TiO_2 nanoparticles agglomerated, as shown by scanning electron microscopy (SEM) images. All scattered particles with a size less than 17 nm were seen in these images. By using SEM analysis, TiO_2: piperine NPs are in a spherical shape with small pores and normally found in the cluster that forms the bunch type surface (Fig. 2(b)).

Transmission Electron Microscope (TEM) images of TiO_2 samples

TEM images were used to assess the morphology, crystallinity, and size of synthesized TiO_2 and TiO_2: piperine nanoparticles. The shape of the nanoparticles was spherecial and small size variance (see Fig. 3). The scale was between 10 and 20 nanometers. The nanoparticles were found to be 15 nm in size on average. Synthesized TiO_2 and TiO_2: piperine

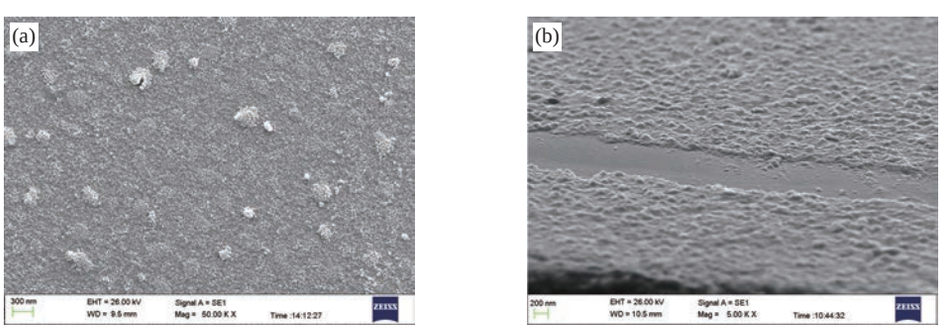

Fig. 2 (a) SEM results for TiO_2 nanoparticles; **(b)** SEM results for TiO_2: piperine nanoparticles.

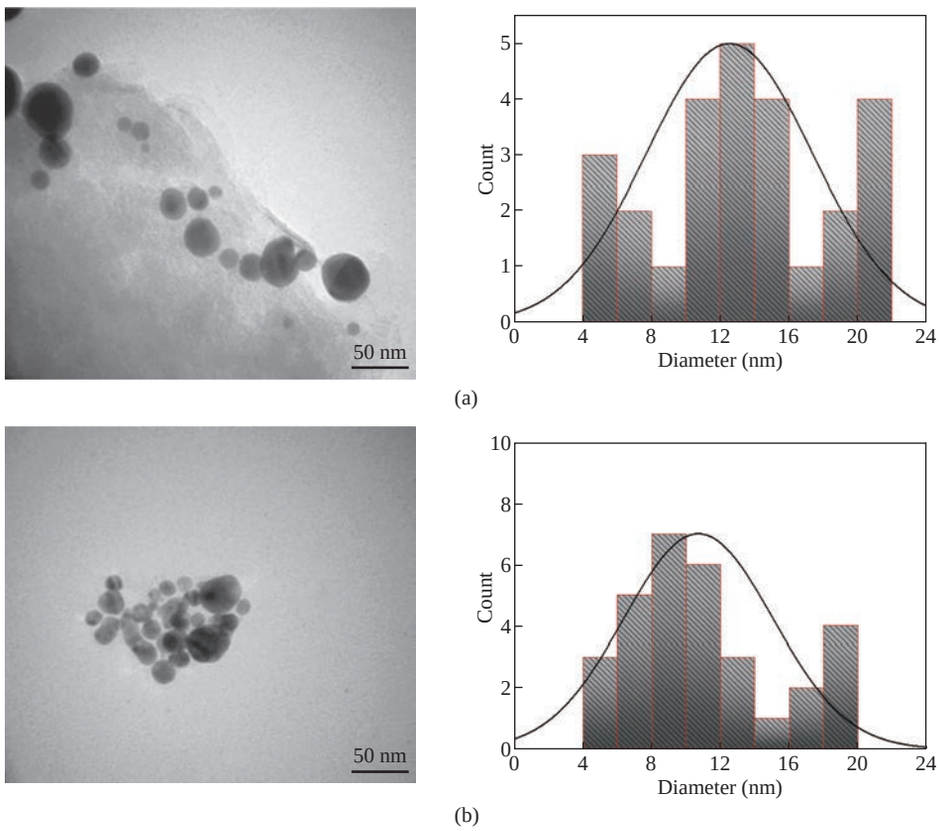

Fig. 3 TEM results for **(a)** TiO_2 and **(b)** TiO_2: piperine nanoparticles.

nanoparticles are in anatase process with strong crystallinity and dotted concentric circles, which can be assigned to the spherical form of TiO_2, as determined by XRD analysis. All of this is depicted in Fig. 3. The diameter of the TiO_2 particles was noticed to be smaller for piperne modified TiO_2 nanoparticles (8-10 nm) (Fig. 3(b)) as compared to chemically prepared TiO_2. The TEM results were found to be ingood agreement with the XRD measurements.

EDXS results of TiO_2 samples

EDX analysis was used to determine the elemental composition of the TiO_2 nanostructure, as shown in the Fig. 4. The EDX study of the nanoparticle (installed in SEM) reflects the atomic percentage (percentage) of elements such as Ti and O, which are clearly visible in the images with a ratio of 83:17 and no other peaks are observed this confirm the presence of TiO nanoparticles.

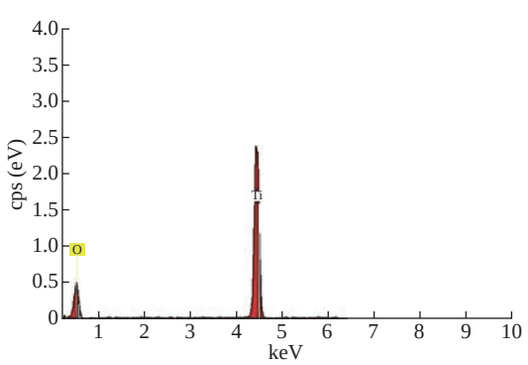

Fig. 4 EDXS results for TiO_2 nanoparticles.

Absorption

The effect of growing conditions on the optical properties of prepared films has been thoroughly investigated. Figure 5(a) and 5(b) shows that the UV-Vis absorption spectrum of TiO_2 and TiO_2: piperine nanoparticles solution has an absorption edge in the range of (340-355) nm, suggesting that the TiO_2 colloidal solution obtained is anatase phase. The band gap energies (E_g) of the prepared TiO_2 nanoparticles (3.46 eV) are higher than the value of (3.2 eV) for bulk TiO_2, as shown in Fig. 5. This can be explained by the fact that the band gap of semiconductors is particle size dependent. The band distance widens as particle size decreases, and the absorption edge shifts to a higher energy (blue shift) as particle size decreases. The absorption onset of the present samples can be attributed to the direct transfer of electrons in TiO_2 nanocrystals, based on the blue change of the absorption location from bulk TiO_2. The absorption spectrum of UV-Visible (wavelength versus

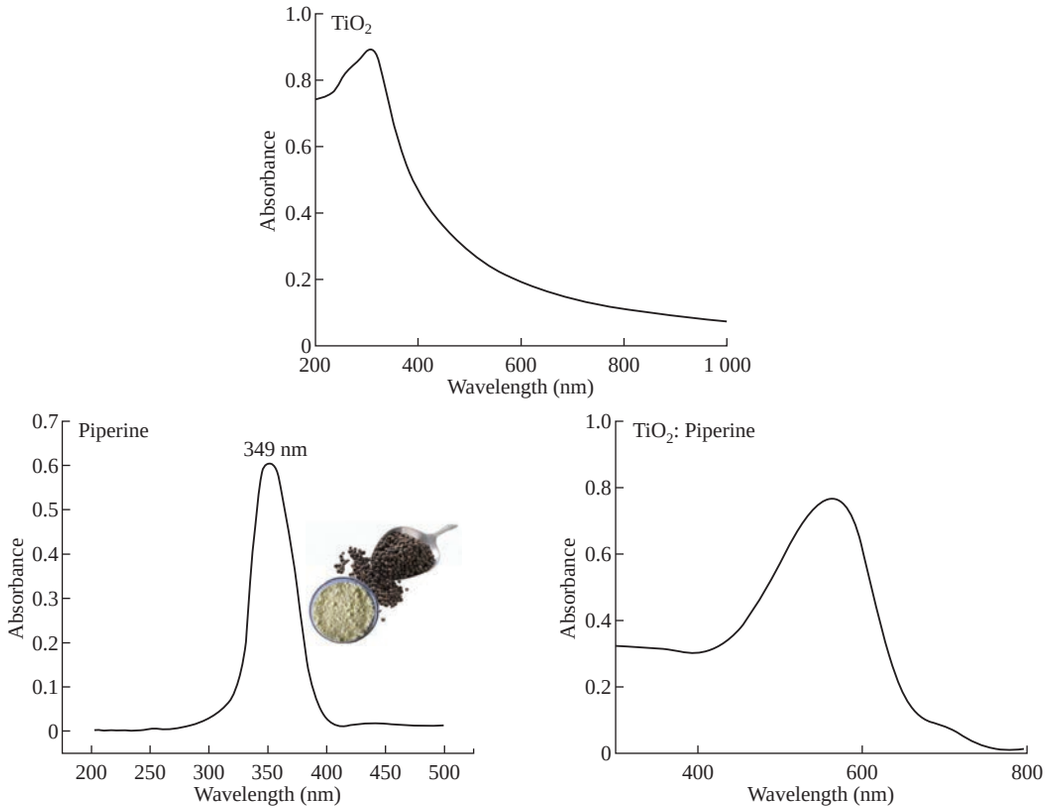

Fig. 5 Absorption results for TiO_2, piperine and TiO_2: piperine nanoparticles.

absorbance) exhibits two peaks at wavelength of 260 nmand 325 nm, that its unique of TiO_2 NPs well in an agreement with the reported results [35, 36]. UV-vis spectroscopy has also been used for the confirmation of TiO_2 NPs formation in aqueous solution.

Fourier transformation-Infrared spectroscopy (FTIR) results of TiO_2 nanoparticles

The results of Fourier transformation-Infrared spectroscopy provide detail. About the structure of the phases and how oxygen binds to metal ions. The FTIR spectra of TiO_2 nanoparticles are shown in the figure below (see Fig. 6). The peaks in the FTIR spectrum of TiO_2 nanoparticles corresponding to 3454 cm^{-1} are due to the stretching of the H-bond of the O-H (Alcohol) group, as shown in Fig. 6. C=C corresponds to the peaks seen at 1627 cm^{-1} and 1419 cm^{-1} (medium weak multiple bands). The stretching and vibration modes of O–Ti–O are shown in the TiO_2 sample by the peaks corresponding to 665cm^{-1} and 648 cm^{-1}. As Ti atoms collide with oxygen, the mean kinetic energy of the Ti atoms decreases, resulting in the formation of (O^{+2}) ions (through energetic change reaction of Ti with O_2 molecules). As a result, chemical bonding such as (O–Ti–O) stretching modes are formed.

This absorption peak in between the wavenumber range 650-700 cm^{-1} is the characteristic peak of

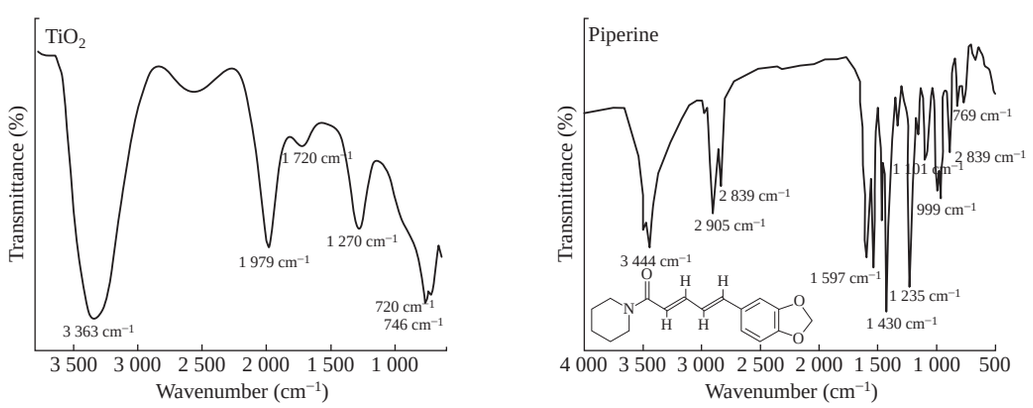

Fig. 6 FTIR results for TiO_2 nanoparticles and piperine.

TiO_2 NPs anatase phase as cited in the literature [26, 37]. The peaks appearing in between the range of 1000-1300 cm^{-1} can be associated to mainly Ti–O–Ti vibrations which clearly showed O–Ti–O bond. According to literature, the FTIR spectrum of TiO_2 nanomaterials prepared with and without CHE present similar FTIR spectra with peak around 450 cm cm^{-1} assigned to stretching vibration of Ti–O–Ti bonds. The broad band at 3428 cm^{-1} can be ascribed to the –OH stretching vibration of the adsorbed water molecules on TiO_2 surface and the peak around 1630 cm^{-1} is attributed to the bending vibrations of –OH.

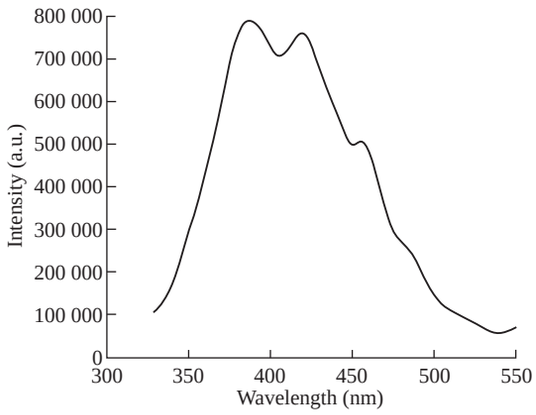

Fig. 7 PL spectra for TiO_2 nanoparticles.

PL spectra

To study the separation efficiency of photogenerated electrons and holes, the room temperature PL spectra of the as-synthesized composite structure TiO_2 were carried out, respectively. Figure 7 exhibits the PL spectra of all samples. The decrease of PL intensity indicates the efficient electron-hole separation and long-lived carriers.

Antibacterial Activity of Nanoparticles

The antibacterial activity of the nanoparticles was investigated using *S. aureus* and *E. coli*. The zones of inhibition after exposing the organisms to different concentrations of nanoparticles were measured and presented in Figs. 8(a) and 8(b). The antibacterial activity of TiO_2 NPs and TiO_2: piperine was tested on the following Bacteria *S. aureus* and *E. coli*. A figure reveals the zone of inhibition diameter of TiO_2 NPs and TiO_2: piperine NPs on bacteria strains, in which that TiO_2: piperine NPs exhibited higher effect on *E. coli* and *S. aureus*. The inhibition zone increased significantly with increasing the concentration of TiO_2: piperine NPs. *S. aureus* was more sensitive to TiO_2:

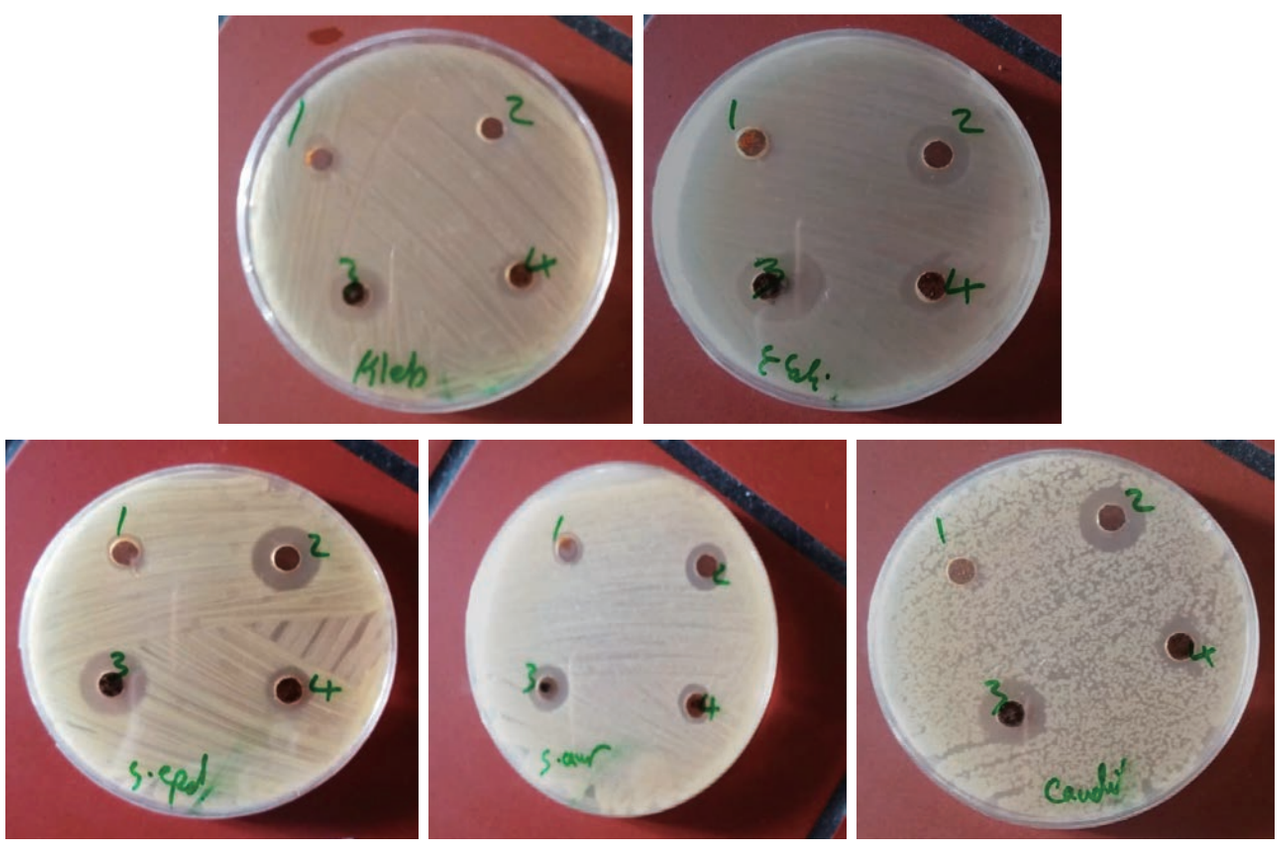

Fig. 8 The antibacterial activity of the nanoparticles was investigated using *S. aureus* and *E. coli* (a) TiO_2 NPs and (b) TiO_2: Piperine NPs.

piperine NPs than *E. coli*. *E. coli* is a Gram-negative bacterium and it is less susceptible to antimicrobials than Gram-positive bacteria like *S. aureus* because it is more resistant to lipophilic and amphiphilic inhibitors than those Gram positive, including dyes, detergents, free fatty acids, antibiotics and chemotherapeutics agents may be attributed to the presence of the outer membrane. The pore channels slowed the penetration of small hydrophilic solutes and the low fluidity of the lipopolysaccharide layer decreased the rate of Trans membrane diffusion of lipophilic solutes.

Conclusions

The synthesize of TiO_2 NPs characterized by SEM, TEM, FE-SEM, EDX, various results confirmed the spherical shape and clustered form of TiO_2 NPs. SEM images TiO_2 sample prepared chemically showed agglomeration of TiO_2 particles comparing to piperene modified TiO_2 particles. The diameter of the TiO_2 particles was noticed to be smaller for piperne modified TiO_2 nanoparticles (8-10 nm) as compared to chemically prepared TiO_2. The TEM results were found to be ingood agreement with the XRD measurements. The intensities difraction peak decreases and becomes broader for TiO_2: piperine nanoparticles indicating smaller particle size which is important for quality and decreasing TiO_2 tixiocity.

Conflict of Interests

The authors declare that no competing interest exists.

References

[1] Zeynep Busra Bolat, Zeynep Islek, Bilun Nas Demir, Elif Nur Yilmaz, Fikrettin Sahin and Mehmet Hikmet Ucisik, Curcumin- and Piperine-Loaded Emulsomes as Combinational Treatment Approach Enhance the Anticancer Activity of Curcumin on HCT116 Colorectal Cancer Model, *Front. Bioeng. Biotechnol.*, 2020, 11 February.

[2] W. Li, Chaoying Ni, Hangyu Lin, C.P. Huang and Syed Ismat Shah, Size Dependence of Thermal Stability of TiO_2 Nanoparticles. *Journal of Applied Physics*, 2004, 96(11): 6663.

[3] Hengzhong Zhang and Jillian F. Banfield. New kinetic model for the nanocrystalline anatase-torutile transformation revealing rate dependence on number of particles. *Am. Mineral*. 1999, 84: 528.

[4] Athanassios Tsevis, Nikos Spanos, Petros G. Koutsoukos, Ab J. van der Linde and Johannes Lyklema. Preparation and characterization of anatase powders. *J. Chem. Soc., Faraday Trans*, 1998, 94(2): 295.

[5] M.R. Ranade, A. Navrotsky, H.Z. Zhang, J.F. Banfield, S.H. Elder, A. Zaban, P.H. Borse, S.K. Kulkarni, G.S. Doran and H.J. Whitfield, (Energetics of nanocrystalline TiO_2) PNAS99, 2002: 6476.

[6] J. Arbiol, J. Cerda, G. Dezanneau, A. Cirera, F. Peiro, A. Cornet and J.R.Mornate, (Effects of Nb doping on the TiO_2 anatase-to-rutile phase transition). *Journal Of Applied Physics*. 2002, 92: 853.

[7] Kazuya Nakataa, Tsuyoshi Ochiaia, Taketoshi Murakamia, Akira Fujishimaa, Photoenergy conversion with TiO_2 photocatalysis: new materials and recent applications, *Electrochim. Acta*, 2012, 84: 111-103.

[8] Wenjuan Tan, Jose R. Peralta-Videa and Jorge L. Gardea-Torresdey Interaction of titanium dioxide nanoparticles with soil components and plants: current knowledge and future research needs–a critical review, Environ. *Sci. J. Integr. Environ. Res. Nano*. 2018, 5(2): 257-278.

[9] Wenzhang Fang, Mingyang Xing, Jinlong Zhang, Modifications on reduced titanium dioxide photocatalysts: a review, *J. Photochem. Photobiol. C Photochem. Rev*. 2017, 32: 21-39.

[10] Chouirfa H., Bouloussa H., Migonney V., Falentin-Daudré C., Review of titanium surface modification techniques and coatings for antibacterial applications, *Acta Biomater*. 2019, 83: 37-54.

[11] Adawiyah J. Haider, Zainab N. Jameel, Imad H. Al-Hussaini, Review on: titanium dioxide applications, *Energy Procedia*, 2019, 157: 17-29.

[12] Maja Vujovic, Emilija Kostic, Titanium dioxide and zinc oxide nanoparticles in Sunscreens: a review of toxicological data, *J. Cosmet. Sci*., 2019, 70(5): 223-234.

[13] Grande, F., Tucci, P. Titanium dioxide nanoparticles: a risk for human Health Mini Rev. Med. Chem. 2016, 16: 762-769.

[14] Shi, J., Yang, D., Jiang, Z., Jiang, Y., Liang, Y., Zhu, Y. Simultaneous size control and surface functionalization of titania nanoparticles through bioadhesion-assisted bio-inspired mineralization. *J. Nanopart. Res*., 2012, 14(9): 1120.

[15] Narkevica, I., Stradina, L., Stipniece, L., Jakobsons, E., Ozolins, J. Electrophoretic deposition of nanocrystalline TiO_2 particles on porous TiO_2-X ceramic scaffolds for biomedical applications. *J. Eur. Ceram. Soc*., 2017, 37(9): 3185-3193.

[16] Mollavali, M., Falamaki, C., Rohani, S. Efficient light harvesting by NiS/CdS/ZnS NPs incorporated in C, N-co-doped-TiO_2 nanotube arrays as visible-light sensitive multilayer photoanode for solar applications. *Int. J. Hydrog. Energy*, 2018, 43: 9259-9278.

[17] Pant, B., Park, M., Park, S.J. TiO_2 NPs assembled into a carbon nanofiber composite electrode by a one-step electrospinning process for supercapacitor applications. *Polymers*, 2019, 11(5): 899.

[18] Irshad, M.A., Nawaz, R., ur Rehman, M.Z., Imran, M., Ahmad, M.J., Ahmad, S., Ali, S. Synthesis and characterization of titanium dioxide nanoparticles by chemical and green methods and their antifungal activities against wheat rust. *Chemosphere*, 2020, 258: 127352.

[19] Muhammad Atif Irshad, Rab Nawaz, Muhammad Zia ur Rehman, MuhammadAdrees, Muhammad Rizwan, Shafaqat Ali a.d., Sajjad Ahmad, Sehar Tasleem, Synthesis, characterization and advanced sustainable applications of titanium dioxide nanoparticles: A review. *Ecotoxicology and Environmental Safety*, 212(2021): 111978.

[20] Sharma, R., Sarkar, A., Jha, R., Kumar Sharma, A., Sharma, D. Sol-gel-mediated synthesis of TiO_2 nanocrystals: structural, optical, and electrochemical properties. *Int. J. Appl. Ceram. Technol*., 2020, 17(3): 1400-1409.

[21] Ramakrishnan, V.M., Natarajan, M., Santhanam, A.,

Asokan, V., Velauthapillai, D. Size controlled synthesis of TiO_2 nanoparticles by modified solvothermal method towards effective photo catalytic and photovoltaic applications. *Mater. Res. Bull*., 2018, 97: 351-360.

[22] Horti, N., Kamatagi, M., Patil, N., Nataraj, S., Sannaikar, M., Inamdar, S. Synthesis and photoluminescence properties of titanium oxide (TiO_2) nanoparticles: effect of calcination temperature. Optik, 2019, 194: 163070.

[23] Wang, Z., Haidry, A.A., Xie, L., Zavabeti, A., Li, Z., Yin, W., Fomekong, R.L., Saruhan, B. Acetone sensing applications of Ag modified TiO_2 porous nanoparticles synthesized via facile hydrothermal method. *Appl. Sur. Sci.*, 2020, 533: 147383.

[24] Subhapriya, S., Gomathipriya, P. Green synthesis of titanium dioxide (TiO_2) nanoparticles by Trigonella foenum-graecum extract and its antimicrobial properties. *Microb. Pathog.*, 2018, 116: 215-220.

[25] Abisharani, J.M., Devikala, S., Kumar, R.D., Arthanareeswari, M., Kamaraj, P. Green synthesis of TiO_2 nanoparticles using Cucurbita pepo seeds extract. *Mater Today Proc*., 2019, 14: 302-307.

[26] Irshad, M.A., Nawaz, R., Ur Rehman, M.Z., Imran, M., Ahmad, M.J., Ahmad, S., Ali, S. Synthesis and characterization of titanium dioxide nanoparticles by chemical and green methods and their antifungal activities against wheat rust. *Chemosphere*, 2020, 258: 127352.

[27] Marwa Abdul Muhsien Hassan, Abdul Kader S. Abdul Kader and Rana Ismael Khaleel, Construction of Nanobiomaterials using Chemical Method, IOP Conf. Series: Materials Science and Engineering, 928(2020): 072067.

[28] Esfahani, R.N., Khaghani, S., Azizi, A., Mortazaeinezhad, F., Gomarian, M. Facile and eco-friendly synthesis of TiO_2 NPs using extracts of Verbascum thapsus plant: an efficient photocatalyst for reduction of Cr(VI) ions in the aqueous solution. *J. Iran. Chem. Society*, 2020, 17(1): 205-213.

[29] Goutam, S.P., Saxena, G., Singh, V., Yadav, A.K., Bharagava, R.N., Thapa, K.B. Green synthesis of TiO_2 nanoparticles using leaf extract of Jatropha curcas L. for photocatalytic degradation of tannery wastewater. *Chem. Eng. J.*, 2018, 336: 386-396.

[30] Pal, S., Tak, Y.K., Song, J.M. Does the antibacterial activity of silver nanoparticles depend on the shape of the nanoparticle? A study of the gram-negative bacterium Escherichia coli. *Appl. Environ. Microbiol.*, 2007, 73(6): 1712-1720.

[31] Gugliotti, L.A., Feldheim, D.L., Eaton, B.E. RNA-mediated control of metal nanoparticle shape. *J. Am. Chem. Soc*., 2005, 127: 17814-17818.

[32] Schuler, E., Gustavsson, A.K., Hertenberger, S., Sattler, K. Solar photocatalytic and electrokinetic studies of TiO_2/Ag nanoparticle suspensions. *Sol. Energy*, 2013, 96: 220-226.

[33] Yeganeh-Faal, A., Bordbar, M., Negahdar, N., Nasrollahzadeh, M. Green synthesis of the Ag/ZnO nanocomposite using Valeriana officinalis L. root extract: application as a reusable catalyst for the reduction of organic dyes in a very short time. *IET Nanobiotechnol*, 2017, 11: 669-676.

[34] Fatimah Al Qarni, Nuhad A. Alomair and Hanan H. Mohamed Environment-Friendly Nanoporous Titanium Dioxide with Enhanced Photocatalytic Activity. *Catalysts*, 2019, 9: 799; doi: 10.3390/catal9100799.

[35] Maar, R.R., Zhang, R., Stephens, D.G., Ding, Z., Gilroy, J.B. Near-infrared photoluminescence and electrochemiluminescence from a remarkably simple boron difluoride formazanate dye. *Angew. Chem. Int. Ed*., 2019, 58 (4): 1052-1056.

[36] Solano, R.A., Herrera, A.P., Maestre, D., Cremades, A. Fe-TiO_2 nanoparticles synthesized by green chemistry for potential application in waste water photocatalytic treatment. *J. Nanotechnol.*, 2019: 1-11.

[37] Sethy, N.K., Arif, Z., Mishra, P.K., Kumar, P. Green synthesis of TiO_2 nanoparticles from Syzygium cumini extract for photo-catalytic removal of lead (Pb) in explosive industrial wastewater. *Green Process. Synth.*, 2020, 9(1): 171-181.